Electronic Supporting Information (ESI)

Observation of bending, cracking and jumping phenomena on cooling and heating of Tetrahydrate Berberine Chloride crystals

Manjeet Singh,[a] Subhrajyoti Bhandary,[a] Rohit Bhowal,[a] and Deepak Chopra[a]*

[a] Crystallography Crystal Chemistry Laboratory, Department of Chemistry, Indian Institute of Science Education and Research Bhopal, Bhopal By-Pass Road Bhauri, Bhopal-462066, Madhya Pradesh, India.Email: dchopra@iiserb.ac.in

Experimental Methods:

Crystallizations of tetrahydrated and dihydrated berberine chloride

Berberine chloride was purchased from Sigma-Aldrich Company and has been used without further purification. The single crystals of the tetrahydrated phase (BL-4H_2O) were obtained during the mechanical and liquid-assisted grinding of berberine chloride with the additive pyrene (was purchased from Sigma-Aldrich Company) by taking 1:1 stoichiometric ratio of BL (32.3 mg, 0.087 mmol) and PY (17.7 mg, 0.087 mmol), using an agate mortar and pestle. Methanol was used as a solvent for grinding. The initial mixture was grinded for ~ 15 minutes without any solvent. Then grinding was carried out for ~ 30 minutes with the drop-wise addition of solvent, at an interval of 15 minutes each.[1] The resulting powder was air dried and crystallized using various solvents of HPLC grade in 5.0 ml beakers and then kept for crystallization at room temperature (25°C). The slow evaporation of Berberine chloride from acetonitrile solvent at room temperature results in the formation of single crystals of the dihydrated phase (BL-2H_2O). These obtained crystals were then characterized structurally using SCXRD and then these crystals were further used for the purpose of investigation of the phase transition and all other related characterizations.

Single Crystal X-ray Diffraction (SCXRD)

The single crystal X-ray diffraction measurements for BL-4H_2O andBL-2H_2O crystal were carried out on a Bruker APEX II Kappa CCD and D8 Venture diffractometer equipped with a graphite monochromator using MoKα radiation (λ = 0.71073 Å) at 100(2) K and 110 K respectively. Unit cell measurement, data collection, integration, scaling and absorption corrections was performed using Bruker APEX II software.[2]Multiscan absorption corrections were applied using SADABS.[3] The structures were solved by direct methods using SHELXS-97[4] and refined with Full-matrix least squares method using SHELXL-2014[5] present in the program suite WinGX.[6] All non-hydrogen atoms were refined anisotropically, and all hydrogen atoms bound to carbon were placed in the calculated positions using a riding model and all hydrogen atoms bound to oxygen (water) were located from the difference fourier map. All O-H distances for water molecules were fixed to their targeted position. Geometrical calculations were done using PARST[7] and PLATON.[8]The packing diagrams of the molecules were generated using Mercury 3.6 software.[9]

Differential Scanning Calorimetry (DSC) and Thermogravimetric analysis (TGA)

The DSC traces of BL-4H_2O crystal was recorded by using a Perkin-Elmer DSC 6000 instrument under nitrogen gas atmosphere. A sample of precisely weighed about 1.0 to 2.0 mg was placed in non-hermetic sealed aluminium pan in vacuum. The samples were scanned at a rate of 5 °C/min in the range of 30–0°C and 0°C–300 °C under a dry nitrogen atmosphere at a flow rate of 20 ml/min. Thermogravimetric analysis was performed under a mixture of dry air and nitrogen. The amount of material used in TGA ranged from approximately 3.0 mg to 5.0 mg. The temperature was typically increased at a heating rate of 10 °C/min.

Variable Temperature Powder X-Ray Diffraction (VT-PXRD)

The variable temperature powder X-ray diffraction patterns of BL-4H_2O crystals were recorded on a PANalytical Empyrean X-ray diffractometer with CuKα radiation (1.5418 Å). The crystals of BL-4H_2O were placed on a silica sample holder and measured by a continuous scan between 5 to 50° in 2θ with a step size of 0.013103°. Two sets of experiments were performed. In the first one, the sample was cooled from 25 to 15 °C at a cooling rate of 1 °C/min. In the second set, the sample was heated from 10 to 45 °C at a heating rate of 1 °C/min.

Hot Stage Microscopy (HSM)

Hot Stage Microscopic (HSM) experiments were performed on a stereomicroscope equipped with a cool stage apparatus (operating at a cooling rate of 1 and 2°C/min with lnp 10) as well as hot stage apparatus (operating at a heating rate of 1 and 2°C/min), and the photographs were taken with a Leica polarizing microscope. The single crystal was placed on a glass slide and the images of the performed experiments were recorded.

Table S1.SCXRD Data of BL-4H_2O and BL-2H_2Ophases on freshly grown crystals.

	BL-4H_2O	**BL-2H_2O**
Temperature	100 K	110 K
Crystal system	Triclinic	Monoclinic
Space group	*P*-1	*C*2/*c*
M. F.	$C_{20}H_{18}NO_4^+Cl^-.4H_2O$	$C_{20}H_{18}NO_4^+Cl^-.2H_2O$
M. Wt.	443.87	407.83
CCDC	1565650	1811915
a (Å)	6.891(4)	27.449 (7)
b (Å)	11.479(6)	7.0744 (17)
c (Å)	13.142(7)	21.677(6)
α	76.205(4)	90
β	89.221(4)	117.695 (7)
γ	85.231(4)	90
V (Å)	1006.0(10)	3727.1 (16)

Z	2	8
D_{cal}(Mgm^{-3})	1.111	1.454
μ (mm^{-1})	0.239	0.244
F (000)	468	1712
θ (min, max)	1.83, 25.06	2.99, 24.99
$h_{min,\ max}$, $k_{min,\ max}$, $l_{min,\ max}$	(-8, 8), (-13,13), (-15, 15)	(-32, 30), (-8,8), (-20, 25)
No. of ref.	13968	13186
No. of unique ref./ obs. Ref.	3562, 2267	3291, 1742
No. parameters	349	265
R_all, R_obs	0.1034, 0.0578	0.1602, 0.0668
wR2_all, wR2_obs	0.1735, 0.1403	0.1273, 0.1078
$\Delta\rho_{min,\ max}$ (eÅ^{-3})	-0.368, 0.484	-0.375, 0.356
G.o.F	1.021	1.023

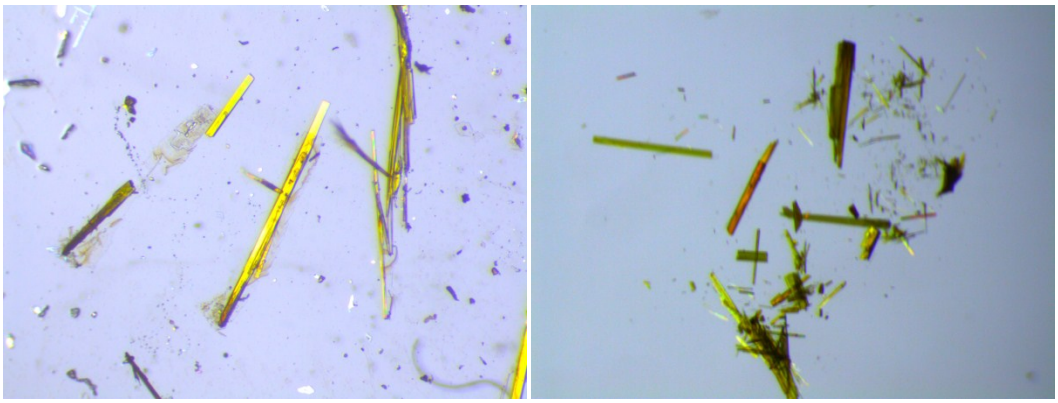

Fig. S1 Photographs of BL-4H_2O crystals

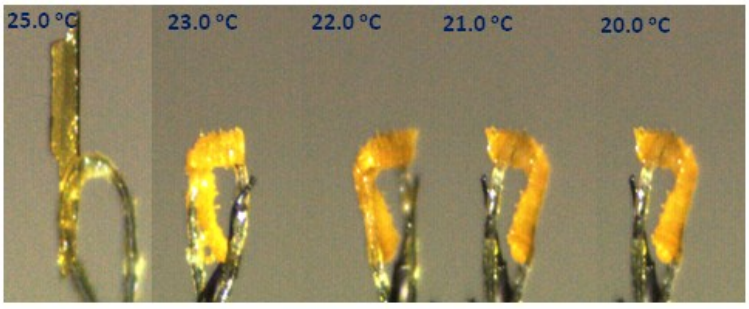

Fig. S2 Snapshots of BL-4H_2O crystal during the cooling from 25 to 20 °C at the rate of 1 °C/min on the X-Ray diffractometer.

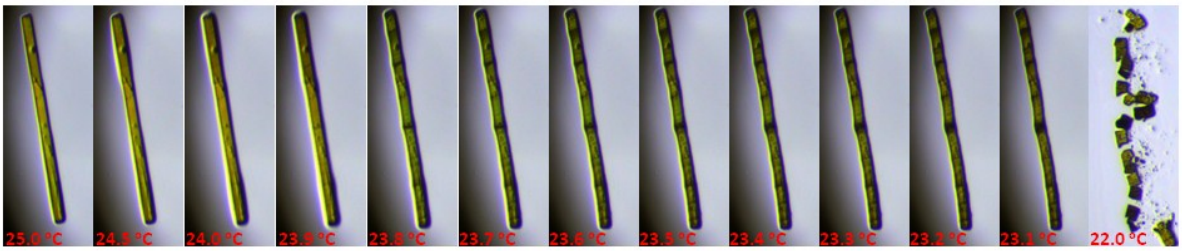

Fig. S3 HSM snapshots at 1 °C/min cooling rate of BL-4H_2O crystal from 25 to 20 °C.

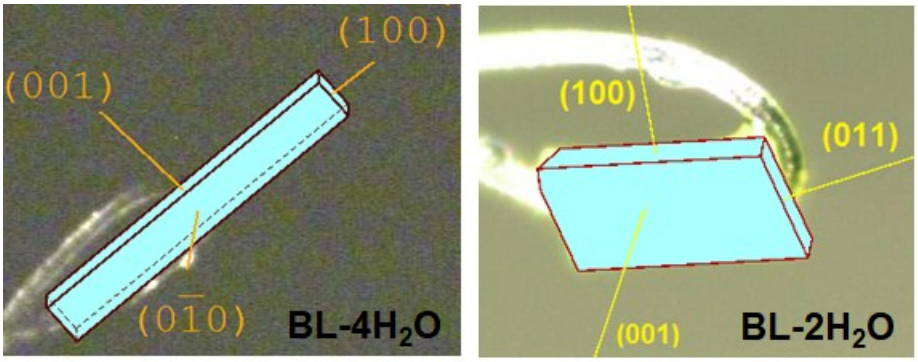

Fig. S4 Experimental face indexing of BL-4H_2O and BL-2H_2O crystalin SCXRD.

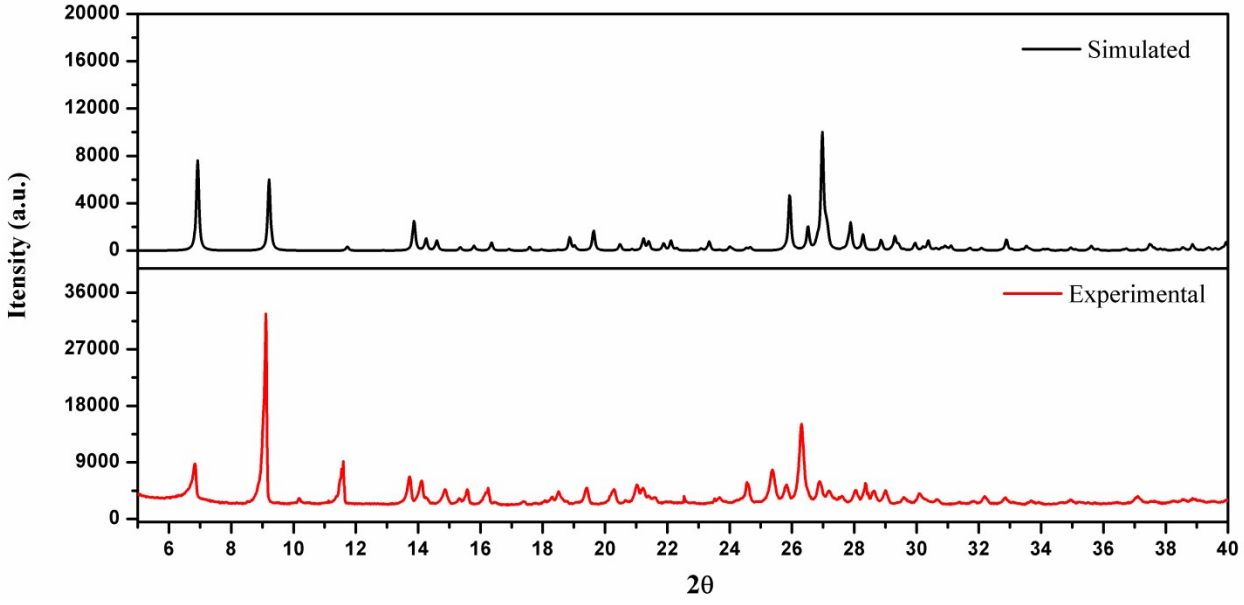

Fig. S5 Experimental and simulated PXRD pattern of BL-4H_2O powdered crystals at room temperature.

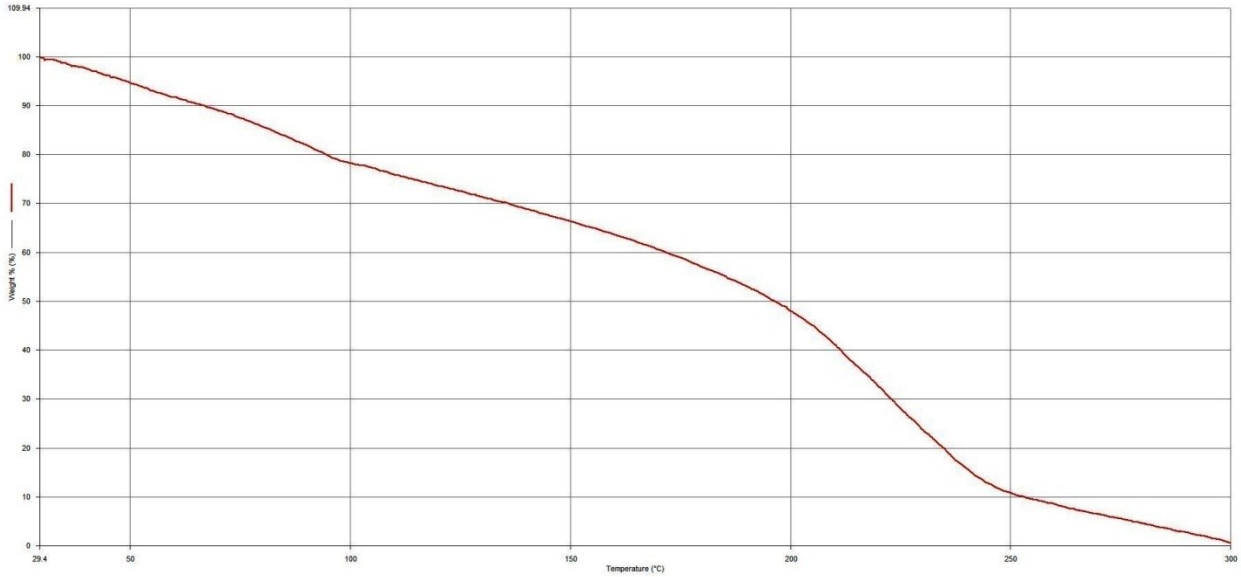

Fig. S6 TGA plot of BL-4H_2O crystals at the rate of 10 ^oC/min.

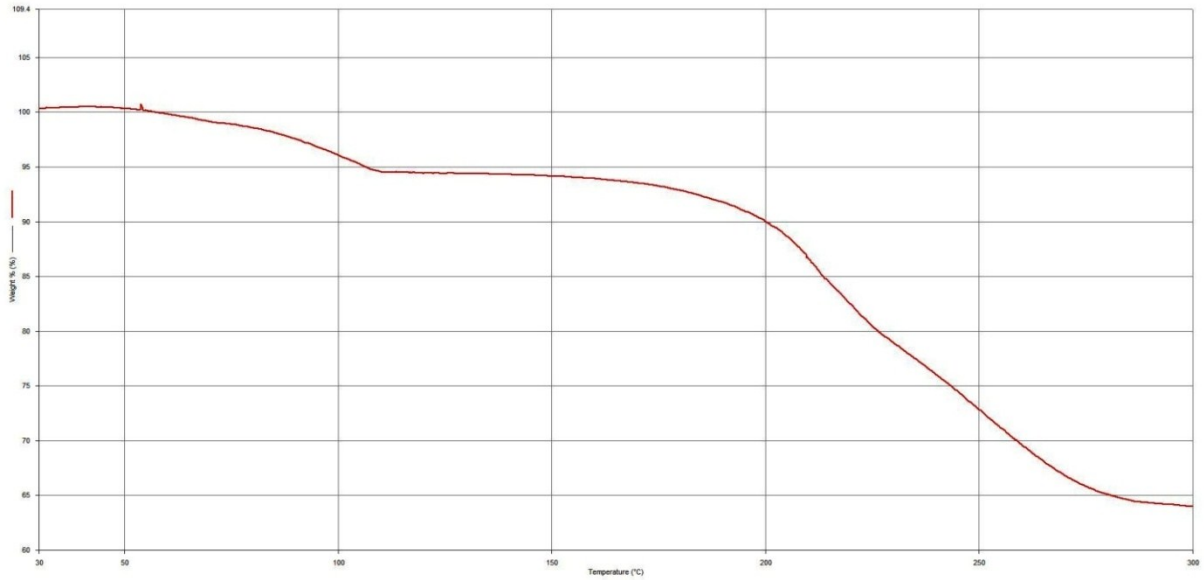

Fig. S7 TGA plot of BL-2H_2O crystals (recovered sample after VT-PXRD) at the rate of 10 ^oC/min.

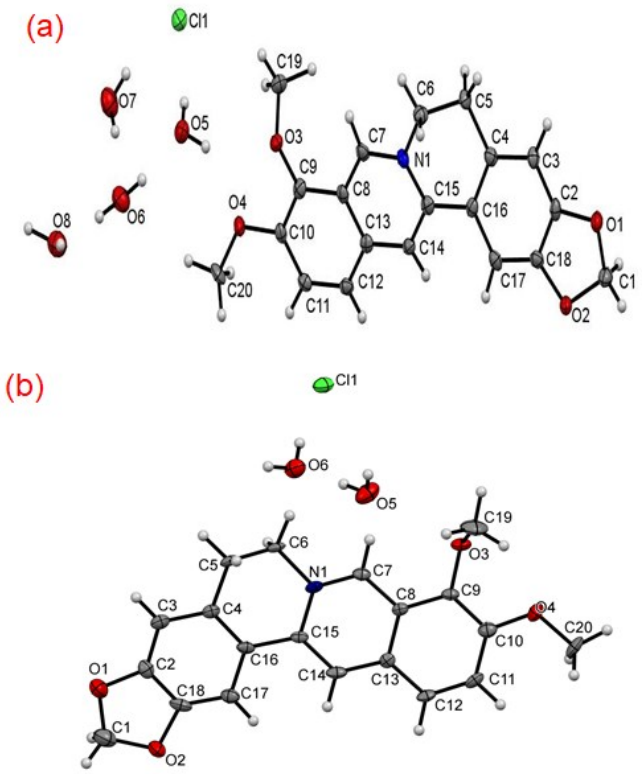

Fig. S8 *ORTEP* representations of the asymmetric unit (50% ellipsoidal probability)for(a)BL-4H_2O and(b) BL-2H_2O with atom numbering scheme.

Table S2. List of intermolecular interactions in Berberine Chloride tetrahydrate (BL-4H_2O).

Interactions	**Symmetry**	**Geometry**		
		D…A (Å)	**H…A (Å)**	**D–H...A (º)**
C20–H20A…O6	x, y, z	3.568	2.584	151
O5–H5C…O3		3.069	2.206	153
O5–H5C…O4		3.016	2.347	128
O5–H5D…$Cl1^-$		3.151	2.225	169
O6–H6C…O5		2.774	1.850	168
O6–H6D…O8		2.752	1.822	171
O7–H7A…$Cl1^-$		3.055	2.144	163
O7–H7B…O6		2.738	1.804	174

$Cl1^-$–H11…O8	-x, -y+1, -z	3.359	2.380	150
C3–H3…O6	x, +y-1, +z+1	3.365	2.516	135
C5–H5A…O7		3.630	2.751	138
C19–H19A…O3	-x, -y+1, -z+1	3.459	2.608	135
C7–H7…O5		3.273	2.273	153
C6–H6B…O5		3.342	2.478	136
C5–H5B…O7	-x+1,-y+1,-z+1	3.842	2.892	147
C19–H19B…$Cl1^-$		3.831	2.774	166
C19–H19A…O2	x,+y+1,+z	3.263	2.705	112
C20–H20B…O1	-x+1,-y,-z+1	3.491	2.733	127
C1–H1A…O4		3.553	2.808	126
C19–H19C…O2		3.518	2.477	162
C12–H12…$Cl1^-$	x,+y-1,+z	3.712	2.774	145
C14–H14…$Cl1^-$		3.526	2.509	157
O5–H5C…O2	-x,-y,-z+1	3.206	2.754	111
C1–H1B…O5		3.374	2.669	122
O8–H8B…O7	-x,-y+2,-z	2.809	1.891	165
O8–H8A…O7	x-1,+y,+z	2.797	1.869	170

Table S3. List of intermolecular interactions in Berberine Chloride dihydrate (BL-2H_2O).

Interactions	**Symmetry**	**Geometry**		
		D…A (Å)	**H…A (Å)**	**D–H...A (deg)**
C19–H19C…O4	x, y, z	3.155	2.610	111
O5–H5C…O6		2.763	1.832	172
O6–H6C…$Cl1^-$		3.170	2.253	165
C1–H1B…O3	x-1/2,-y+1/2,+z-1/2	3.721	2.874	135
C1–H1A…O5		3.440	2.580	136
C17–H17…O5		3.414	2.342	172

C1–H1B…O4		3.505	2.845	119
C20–H20C…O1	-x+1/2+1,-y+1/2,-z+1	3.468	2.754	123
C12–H12…O6		3.590	2.573	157
C14–H14…O5		3.624	2.612	156
C3–H3…O1	-x+1,-y,-z+1	3.466	2.511	147
C19–H19B…O5		3.665	2.669	153
C6–H6B…Cl1$^-$		3.820	2.792	159
C6–H6B…O6	x,+y-1,+z	3.410	2.825	114
O5–H5D… Cl1$^-$		3.287	2.370	165
C7–H7… Cl1$^-$		3.740	2.829	161
C6–H6B…O6	-x+1/2+1,+y-1/2,-	3.470	2.737	125
O6–H6D… Cl1$^-$	z+1/2+1	3.184	2.251	173
C12–H12…Cl1$^-$	x,-y+1,+z-1/2	3.695	2.909	130
C19–H19A…O4	-x+2,+y,-z+1/2+1	3.576	2.589	152
C19–H19C…O2	-x+1/2+1,-y-1/2,-z+1	3.616	2.681	145

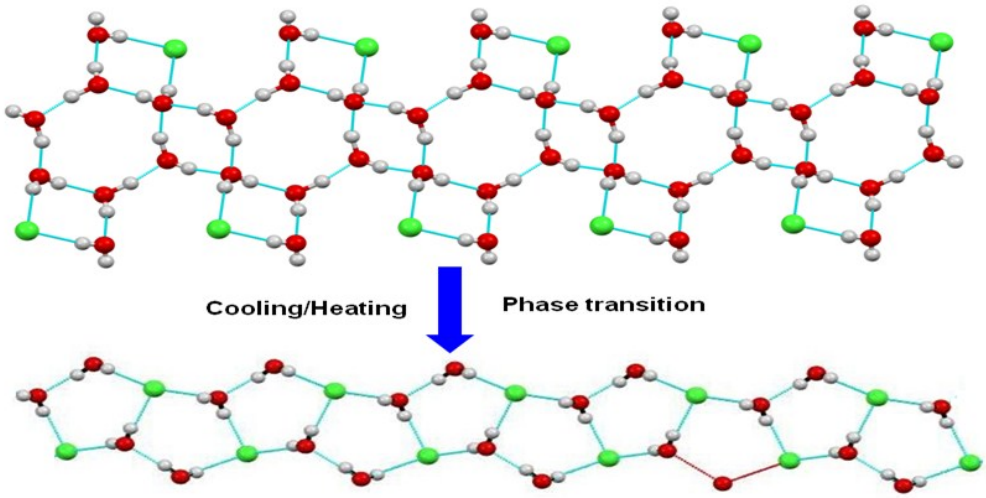

Fig. S9 Rearrangement of fused six and four-membered rings formed by water and chloride ions in BL-4H_2O to fused five-membered rings in BL-2H_2O crystal.

Table S4. Comparisons of unit cell axes of both the forms of berberine chloride crystal

Axes	BL-4H_2O	BL-2H_2O
a	6.8909	(b)$^{\#}$ 7.0935 = $\mathbf{a_1}$
b	11.4787	(a)$^{\#}$ 21.6763/2 = 10.8382 = $\mathbf{b_1}$
c	13.1419	(c)$^{\#}$ 27.5030/2 = 13.7515 = $\mathbf{c_1}$

#: Unit cell representation in the dihydrate

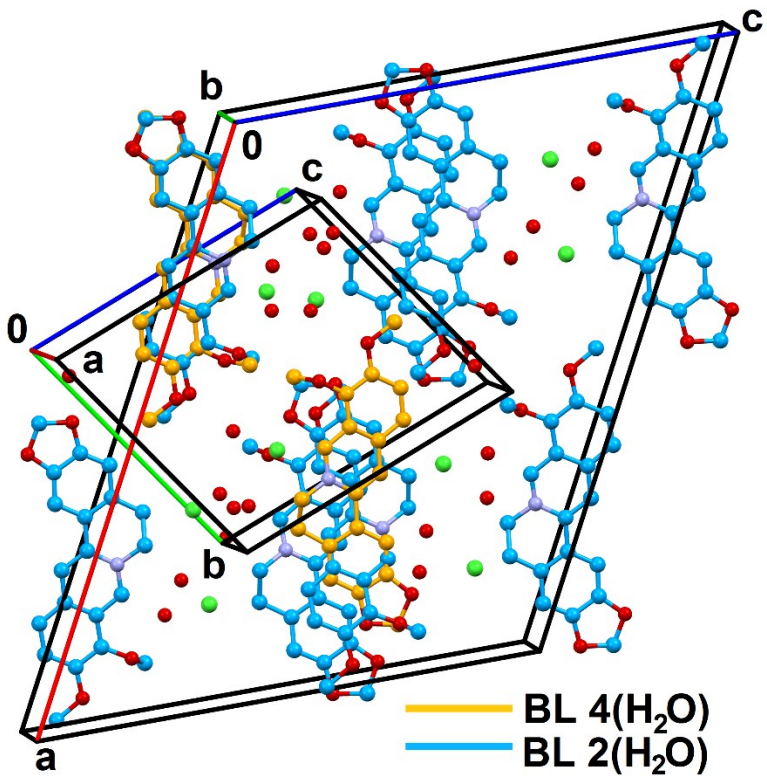

Fig. S10 Overlay of unit cells for the tetrahydrate (triclinic, smaller) and dihydrate (monoclinic, larger) phases showing the interchange of a and b axes preserving the similar c axis with the anisotropic change of cell parameters as indicated in the Table S4.

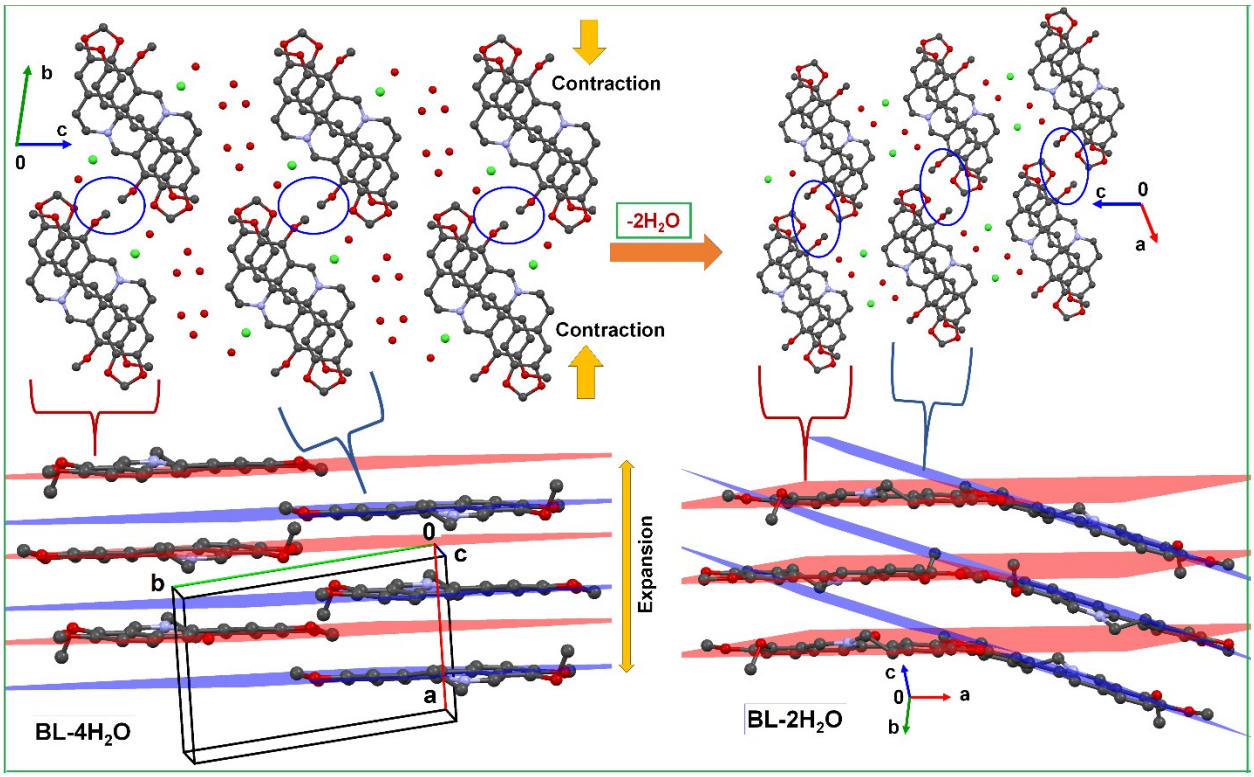

Fig. S11 Structuraltransformationfrom BL-4H_2O (left) to BL-2H_2O (right) showing contraction (see yellow arrows) and movements of layers (see the relative positions of –OMe groups in blue circles). Two such adjacent layers are simultaneously expanded in stacking direction with the reorientation of BL molecules to (see red and blue shading) during the process of conversion.

Energy framework calculations

The energy framework analysis (Reference number 19 in the main manuscript) has been performed using *CrystalExplorer17*[10] to visualize the intermolecular interaction topology in BL-4H_2O and BL-2H_2O phases. The pairwise intermolecular interaction energies are computed using an approach described in (Reference number 19 in the main manuscript). The energies are estimated from B3LYP/6-31G(d,p) molecular wave functions calculated at the crystal geometry, summing up the electrostatic, polarization, dispersion and exchange-repulsion terms based on a scaling scheme. The energy cut-off and tube size are 5 kJ/mol and 80 respectively.

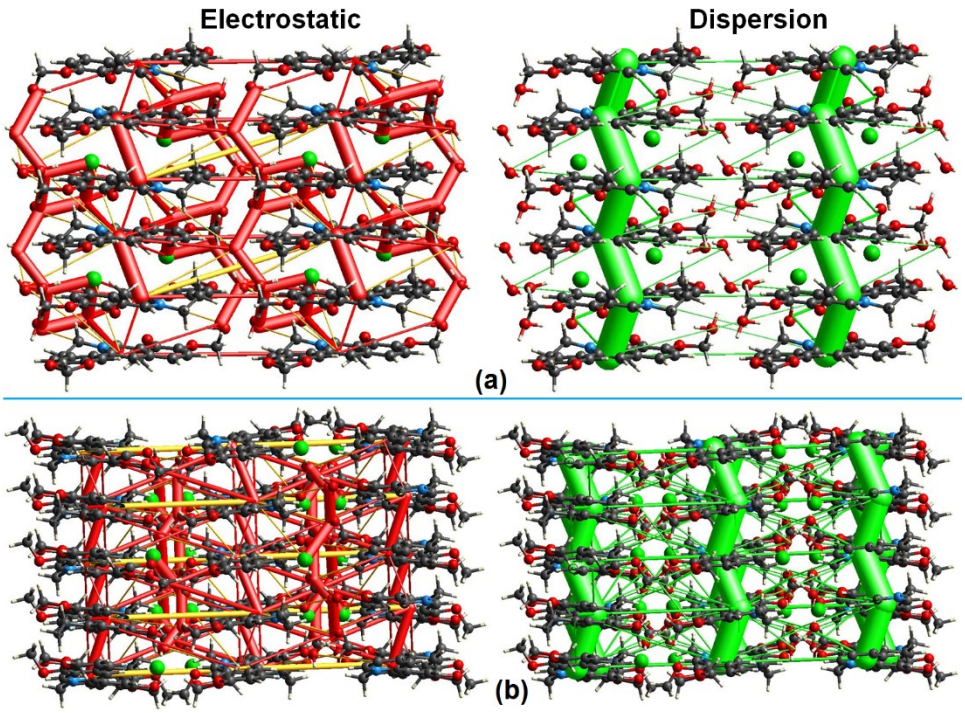

Fig. S12 Energy frameworks corresponding to electrostatic (red) and dispersion (green) components for (a) BL-4H_2O and (b) BL-2H_2O phases.

References:

1. P. K.Mondal, V.Rao, S.Mittapalli and D. Chopra, *Cryst. Growth Des.,*2017,**17,** 1938.
2. APEX2, Version 2 User Manual, M86-E01078; Bruker Analytical X-ray Systems: Madison, WI, USA, 2006.
3. G. M.Sheldrick, SADABS; Bruker AXS: Madison, WI, USA, 2007.
4. G. M. Sheldrick, *ActaCrystallogr.,*2008,**A64**, 112.
5. G. M. Sheldrick, *ActaCrystallogr*.,2015,**A71**, 3.
6. L. J. Farrugia, *J. Appl. Crystallogr*. 1999,**32**, 837.
7. M. Nardelli, *J. Appl. Cryst.,* 1995, **28**, 659.
8. A. L. Spek, *ActaCryst.,* 2009, **D65**, 148-155.
9. C. F. Macrae, I. J.Bruno, J. A.Chisholm, P. R.Edgington, P.McCabe, E.Pidcock,

L.Rodriguez-Monge, R.Taylor, J. Van de Streek andP. A. Wood, *J. Appl. Crystallogr.,* 2008,**41**, 466. (www.ccdc.cam.ac.uk/mercury).

10. M. J.Turner, J. J. McKinnon, S. K.Wolff, D. J.Grimwood, P. R.Spackman, D.Jayatilaka and M. A.Spackman, *CrystalExplorer17*, 2017. University of Western Australia. *http://hirshfeldsurface.net.*